JOURNAL OF COMPUTATIONAL PHYSICS 24, 348–360 (1977)

The Integration of the Vlasov Equation for a Magnetized Plasma

C. Z. CHENG

Plasma Physics Laboratory, Princeton University, Princeton, New Jersey 08540

Received April 29, 1976; revised December 8, 1976

A second-order splitting scheme is developed to integrate the three-dimensional Vlasov equation for a plasma in a magnetic field. In the scheme we divide the integration of the Vlasov equation into a series of intermediate steps and Fourier interpolation and the accurate space derivative method with a third-order Taylor expansion are used to integrate the fractional equations. Numerical experiments related to cyclotron waves in 2 and $2\frac{1}{2}$ D are demonstrated with high accuracy and efficiency.

1. INTRODUCTION

The numerical integration of the Vlasov equation has been intensely studied in recent years [1–6]. However, little progress has been made on fast and accurate integration of the Vlasov equation in two and three dimensions for a magnetized plasma. A knowledge of the nonlinear evolution of the magnetized plasmas in two and three dimensions is indispensible in understanding the plasma physics of controlled thermonuclear fusion.

A splitting scheme for the numerical solution of the one-dimensional Vlasov equation for an unmagnetized plasma has recently been proposed by Cheng and Knorr [6]. In the scheme, the Vlasov equation was integrated in the x–v phase space by splitting up the free streaming term and the acceleration term in such a way that the overall scheme is second order in Δt. Fourier interpolation and spline interpolation were used to integrate the resulting fractional equations, and the scheme was demonstrated to be very accurate and efficient. Another interesting approach for the numerical integration of the Vlasov equation is based on accurate space derivative method in which the derivatives with respect to all the phas space variables are computed by finite Fourier transform methods. The time differencing scheme is a third-order truncated Taylor series expansion of the distribution function in Δt [5]. The approach has the disadvantages that not only the computation becomes very time consuming when there are a number of nonlinear terms in several variables, but also small Δt has to be used due to numerical stability criteria.

In this paper we generalize the splitting scheme [6] to the integration of the three-dimensional Vlasov equation for a magnetized plasma. In the scheme we divide the integration of the Vlasov equation into a series of intermediate steps and the overall

ISSN 0021-9991

scheme is second order in Δt. The resulting fractional equations are computed at each time step with Fourier interpolation and the accurate space derivative method with a third-order Taylor expansion [5]. Since fast Foureir transform is used to do the Fourier interpolation and Gazdag's accurate space derivative calculations, the programming becomes very simple and the accuracy and efficiency are accomplished.

The generalized splitting scheme is described in Section 2. In Section 3 we demonstrate the accuracy and efficiency of the splitting scheme through numerical experiments related to linear and nonlinear cyclotron waves in 2 and $2\frac{1}{2}$ dimensions for a Maxwellian equilibrium plasma. The conclusions are given in Section 4.

2. The Generalized Splitting Scheme

In this section we will present the splitting scheme for integrating the Vlasov equation with external electric and magnetic fields. For simplicity, we consider the case with $\mathbf{B}_{\text{ext}} = B_0\hat{e}_z$, $\mathbf{E}_{\text{ext}} = 0$. The numerical procedure can be generalized to include more complicated problems with external inhomogeneous magnetic fields.

Consider a three-dimensional, electrostatic collisionless electron plasma immersed in a uniform static magnetic field $\mathbf{B}_0 = B_0\hat{e}_z$. The dimensionless forms of the Vlasov–Poisson equations are

$$\frac{\partial f}{\partial t} + \mathbf{v} \cdot \frac{\partial f}{\partial \mathbf{x}} - (\mathbf{E}(\mathbf{x}, t) + \mathbf{v} \times \boldsymbol{\omega}_c) \cdot \frac{\partial f}{\partial \mathbf{v}} = 0, \tag{1}$$

$$\nabla \cdot \mathbf{E} = 1 - \int f(\mathbf{x}, \mathbf{v}, t)\, d\mathbf{v}, \tag{2}$$

where $\omega_c = eB_0/mc\omega_{pe}$ is the ratio of cylcotron frequency to electron plasma frequency ω_{pe}. A periodic boundary condition in $\mathbf{x}$ is assumed. Following the principles of the splitting scheme used in [6, 7], we split Eq. (1) according to the following four-step procedure.

(i) Solve the free streaming equation

$$(\partial f/\partial t) + \mathbf{v} \cdot (\partial f/\partial \mathbf{x}) = 0 \tag{3}$$

for half a time step with the solution

$$f^*(\mathbf{x}, \mathbf{v}) = f^n(\mathbf{x} - (\mathbf{v}\,\Delta t/2), \mathbf{v}) \tag{4}$$

where $f^n(\mathbf{x}, \mathbf{v})$ denotes the distribution at $t = n\,\Delta t$.

(ii) Calculate the electric field from the Poisson equation

$$\nabla \cdot \mathbf{E}^*(\mathbf{x}) = 1 - \int f^*(\mathbf{x}, \mathbf{v})\, d\mathbf{v}. \tag{5}$$

(iii) Integrate the acceleration equation

$$(\partial f/\partial t) - (\mathbf{E}^*(\mathbf{x}) + \mathbf{v} \times \boldsymbol{\omega}_c) \cdot (\partial f/\partial \mathbf{v}) = 0 \tag{6}$$

for a whole time step with the solution

$$f^{**}(\mathbf{x}, \mathbf{v}) = f^*(\mathbf{x}, \mathbf{v}^*) \tag{7}$$

where $\mathbf{v}^*$ is the solution of the characteristics of Eq. (6) and is given by

$$\begin{aligned}
v_x^*(\mathbf{x}) &= E_y^*(\mathbf{x})/\omega_c + \left(v_x - \frac{E_y^*(\mathbf{x})}{\omega_c}\right) \cos \omega_c \Delta t + \left(v_y + \frac{E_x^*(\mathbf{x})}{\omega_c}\right) \sin \omega_c \Delta t, \\
v_y^*(\mathbf{x}) &= -\frac{E_x^*(\mathbf{x})}{\omega_c} + \left(v_y + \frac{E_x^*(\mathbf{x})}{\omega_c}\right) \cos \omega_c \Delta t - \left(v_x - \frac{E_y^*(\mathbf{x})}{\omega_c}\right) \sin \omega_c \Delta t, \\
v_z^*(\mathbf{x}) &= v_z + E_z^*(\mathbf{x}) \Delta t.
\end{aligned} \tag{8}$$

(iv) Solve the free streaming equation $(\partial f/\partial t) + v \cdot (\partial f/\partial \mathbf{x}) = 0$ again for half a time step with the solution

$$f^{n+1}(\mathbf{x}, \mathbf{v}) = f^{**}(\mathbf{x} - (\mathbf{v}\, \Delta t/2), \mathbf{v}). \tag{9}$$

By substituting Eqs. (7) and (4) into Eq. (9) we obtain

$$f^{n+1}(\mathbf{x}, \mathbf{v}) = f^n(\mathbf{x}', \mathbf{v}') \tag{10}$$

with

$$\begin{aligned}
\mathbf{x}' &= \mathbf{x} - (\Delta t/2)(\mathbf{v} + \mathbf{v}'), \\
\mathbf{v}' &= \mathbf{v}^*(\mathbf{x} - (\mathbf{v}\, \Delta t/2)),
\end{aligned} \tag{11}$$

where $\mathbf{v}^*(\mathbf{x})$ is given by (8).

The characteristics of Eq. (1) are given by

$$d\mathbf{v}/dt = -[\mathbf{E}(\mathbf{x}, t) + \mathbf{v} \times \boldsymbol{\omega}_c], \tag{12}$$

$$d\mathbf{x}/dt = \mathbf{v}. \tag{13}$$

Their solution is equivalent to the solution of Eq. (1). Now we are going to integrate Eqs. (12) and (13) from t_n to t_{n+1}. Their solutions, correct to second order in Δt, are given by

$$\mathbf{x}^n = \mathbf{x}^{n+1} - (\Delta t/2)(\mathbf{v}^n + \mathbf{v}^{n+1}),$$

$$v_x^n = \frac{E_y^{n+(1/2)}}{\omega_c} + \left(v_x^{n+1} - \frac{E_y^{n+(1/2)}}{\omega_c}\right)\cos\omega_c \Delta t + \left(v_y^{n+1} + \frac{E_x^{n+(1/2)}}{\omega_c}\right)\sin\omega_c \Delta t,$$

$$v_y^n = -\frac{E_x^{n+(1/2)}}{\omega_c} + \left(v_y^{n+1} + \frac{E_x^{n+(1/2)}}{\omega_c}\right)\cos\omega_c \Delta t - \left(v_x^{n+1} - \frac{E_y^{n+(1/2)}}{\omega_c}\right)\sin\omega_c \Delta t, \tag{14}$$

$$v_z^n = v_z^{n+1} + E_z^{n+(1/2)}\Delta t,$$

where the time centered electric field $\mathbf{E}^{n+(1/2)}$ is evaluated at $\mathbf{x}^{n+(1/2)} = \mathbf{x}^{n+1} - \mathbf{v}^{n+1}(\Delta t/2) + O(\Delta t^2)$.

A comparison between Eqs. (11) and (14) shows that the splitting scheme (3)–(9) is correct to second order in Δt. It is clear that after we have shifted f in the $\mathbf{x}$ space at time $t = 0$ for one half time step, we can integrate f in the $\mathbf{v}$ space for a full time step, then shift f in $\mathbf{x}$ space for a full time step, and so on.

The above procedure can be applied to more complicated situations with magnetic field inhomogeneity and the results remain accurate to second orler in Δt. The proof is straightforward and will not be presented here. Another advantage of this splitting scheme is that it does not depend on periodic boundary conditions, while the Fourier–Hermite transform method is critically dependent upon spatial periodicity.

From the above analysis we see that our scheme depends on the accuracy of the numerical integration of the linear Eqs. (4) and (7). There are acceptable ways of integrating them, such as Fourier and spline interpolation methods [6], ASD method [5, 8], etc. However, the advantage of each method depends upon the geometry and boundary conditions of the system studied. For free streaming Eq. (4) with spatial periodicity, we will use the Fourier interpolation method to do three subsequent 1D shiftings. The Fourier interpolation can be done more efficiently by employing fast Fourier transform. Integrating acceleration Eq. (6) is more difficult. Due to the fact that the electric and magnetic fields accelerate the particles differently, interpolation methods become much more complicated and time consuming in two and three dimensions. Therefore, we will use one more splitting scheme to integrate Eq. (6) (called method 1.)

In method 1, we replace Eq. (6) with the following sequence of equations

$$\frac{\partial f}{\partial t} - \frac{E_y^*}{\omega_c \Delta t}\frac{\partial f}{\partial v_x} + \frac{E_x^*}{\omega_c \Delta t}\frac{\partial f}{\partial v_y} = 0, \tag{15a}$$

$$\frac{\partial f}{\partial t} + \omega_c \frac{\partial f}{\partial \phi} = 0, \tag{15b}$$

$$\frac{\partial f}{\partial t} + \frac{E_y^*}{\omega_c \Delta t}\frac{\partial f}{\partial v_x} - \frac{E_x^*}{\omega_c \Delta t}\frac{\partial f}{\partial v_y} = 0, \tag{15c}$$

$$\frac{\partial f}{\partial t} - E_z^*\frac{\partial f}{\partial v_z} = 0, \tag{15d}$$

where Eqs. (15a), (15c) must be integrated for the time step Δt. The variable ϕ in Eq. (15b) is the azimuthal angle in the v_x–v_y plane.

A formal solution of Eqs. (15a)–(15d) is given by the sequence of shiftings of the distribution

$$f^*(v_x, v_y, v_z) = f^b(v_x + E_y^*/\omega_c, v_y - E_x^*/\omega_c, v_z), \tag{16a}$$

$$f^{**}(v_x, v_y, v_z) = f^*(v_x \cos(\omega_c \Delta t) + v_y \sin(\omega_c \Delta t), v_y \cos(\omega_c \Delta t) - v_x \sin(\omega_c \Delta t), v_z), \tag{16b}$$

$$f^{***}(v_x, v_y, v_z) = f^{**}(v_x - E_y^*/\omega_c, v_y + E_x^*/\omega_c, v_z), \tag{16c}$$

$$f^e(v_x, v_y, v_z) = f^{***}(v_x, v_y, v_z + E_z^* \Delta t), \tag{16d}$$

where b, e denote the initial and the final distribution, respectively. Subsequently, substituting (16d), (16c), (16b) into (16a), we obtain

$$f^e(v_x, v_y, v_z) = f^b(v_x^*, v_y^*, v_z^*)$$

where v_x^*, v_y^*, v_z^*, are given by Eq. (18) and the equivalence between Eqs. (15a)–(15d) and Eq. (6) is obvious.

From Eq. (15b) it seems most natural to use cylindrical coordinate system for the velocity space. Then (15a) and (15c) become

$$\frac{\partial f}{\partial t} + \frac{E_x \sin\phi - E_y \cos\phi}{\omega_c \Delta t} \frac{\partial f}{\partial v} + \frac{E_x \cos\phi + E_y \sin\phi}{\omega_c \Delta t\, v} \frac{\partial f}{\partial \phi} = 0 \tag{17a}$$

and

$$\frac{\partial f}{\partial t} - \frac{E_x \sin\phi - E_y \cos\phi}{\omega_c \Delta t} \frac{\partial f}{\partial v} - \frac{E_x \cos\phi + E_y \sin\phi}{\omega_c \Delta t\, v} \frac{\partial f}{\partial \phi} = 0 \tag{17b}$$

respectively. We will use accurate space derivative method together with the third-order truncation of the Taylor series to integrate (17a) and (17b). Equations (15b) and (15d) will be integrated by employing a one-dimensional Fourier interpolation. The stability and error analysis of using the third-order Taylor series with accurate space derivative method on integrating the convective type equations has been investigated by Gazdag [5, 8]. It has been applied with success in solving several nonlinear partial differential equations including the Vlasov–Poisson system of equations in three phase space variables [5].

We have also applied Gazdag's accurate space derivative method to integrate Eq. (6) directly (called method 2). In cylindrical coordinates, Eq. (6) can be written as

$$\frac{\partial f}{\partial t} - (E_x \cos\phi + E_y \sin\phi) \frac{\partial f}{\partial v} + \left(\frac{E_x \sin\phi - E_y \cos\phi}{v} + \omega_c\right) \frac{\partial f}{\partial \phi} = 0,$$
$$(\partial f/\partial t) - E_z(\partial f/\partial v_z) = 0. \tag{18}$$

However, the stability criteria forces us to use a small time step of integration with this method for the strong magnetic field case. Employing method 1 allows us to use a larger time step because the fast gyration (15b) of the particle has been separated from the slow guiding center drift motion (15a) and (15c). Also by choosing $\omega_c \Delta t = \Delta\phi$, we do not need to perform interpolation to solve (15b). Thus, for the overall computation, method 1 is better than method 2. Of course, the size of the time step Δt must be limited by the sampling theorem for the maximum frequency $\omega_{\max} = \pi/\Delta t$ observable in the system and by the stability criteria of the accurate space derivative method. However if the magnetic field is weak, method 2 becomes superior to method 1. This is because we can use as large a time step for the latter as for the former and the computation effort is less for the latter.

In the following, we will demonstrate the accuracy and efficiency of the splitting scheme by integrating the 2- and 2½-D Vlasov equations.

3. Numerical Results

In this section wei will present the results of integrating the 2- and 2½-D Vlasov equation. The external magnetic field **B** is chosen to lie in the y–z plane with $\mathbf{B} \cdot \hat{e}_z = B\cos\theta$. We use a rectangular mesh in the x–y plane. In the velocity space we use cylindrical coordinates such that $v_\parallel$ is taken along **B** and $\mathbf{v}_x$ along $\hat{e}_x$. No mesh point is placed at the origin and the smallest velocities associated with the mesh points in the $v_\parallel$ direction and $v_\perp$ plane are $\Delta v_\parallel/2$ and $\Delta v_\perp/2$, respectively, as shown in Fig. 1. The computational domain is

$$R = \{(\mathbf{x}, \mathbf{v}) \mid 0 \leqslant x \leqslant L_x, 0 \leqslant y \leqslant L_y, 0 \leqslant \phi \leqslant 2\pi, |v_\parallel| \leqslant v_{\parallel_{\max}}, |v_\perp| \leqslant v_{\perp_{\max}}\}.$$

N_x, N_y, $2N_p$, N_ϕ, and N_r designate the number of mesh points used in the x, y, $v_\parallel$, ϕ, and $v_\perp$ directions, respectively.

(A) 2-D *and* 2½-D *Linearized Cases*

To test the splitting scheme and gain some insight of the numerical system, we first integrate the linearized Vlasov–Poisson system in 2D and 2½ D for one- and two-species plasmas. The equilibrium distribution is a Maxwellian, f_{0j}, with two or three velocity components and the initial condition is

$$f_j(\mathbf{x}, \mathbf{v}, 0) = f_{0j}(\mathbf{v})(1 + A_j \cos \mathbf{k} \cdot \mathbf{x}).$$

The subscript $j = e, i$ refers to electrons and ions. In this linearized case, the acceleration equation can be solved analytically by integrating along the characteristics. For the one-species plasma case, the ions are considered to be an immobile background. Figure 2 shows the power spectrum of the 2-D electron Bernstein modes with $k_\perp \lambda_D = 1.02$, $\omega_{ce}/\omega_{pe} = 1$. The computational parameters are $N_x = N_y = 4$, $N_\phi = N_r = 8$, $N_p = 0$, $\omega_{pe}\Delta t = \pi/4$, $v_{\parallel_{\max}} = 0$, and $v_\perp = 4.0$. The sequence of

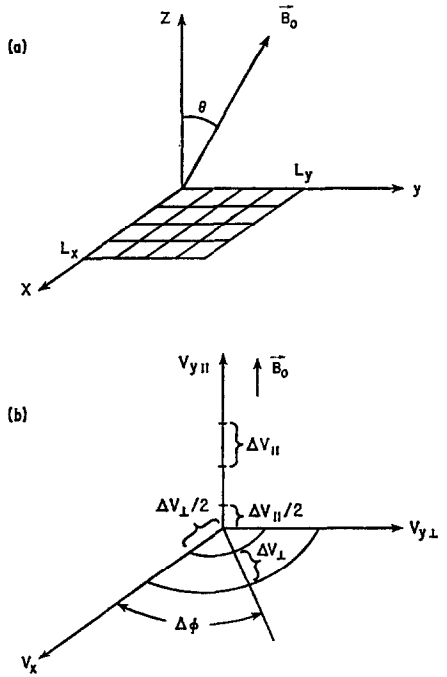

FIG. 1. The $2\frac{1}{2}$ D configuration; (a) shows the spatial domain and (b) shows the computational mesh in the velocity space.

the Fourier mode of potential $\phi(k_\perp, t)$ over 512 time steps was Fourier transformed with respect to time in order to obtain the power spectrum $p(k_\perp, \omega) \propto |\phi(k_\perp, \omega)|^2$. The peaks in Fig. 2 have the values $\omega/\omega_{ce} = 0$, 1.156, 2.125, 3.0625, while the linear theory [9] gives $\omega/\omega_{ce} = 0$, 1.1354, 2.043, 3.005, etc. We should point out the existence of the strong dc mode ($\omega = 0$) in 2-D collisionless magnetized plasmas which was predicted by Hsu and Montgomery [10]. We also note that the recurrence effect, which occurs in the numerical integration of 1-D Vlasov equation for an unmagnetized plasma because of the finite resolution in the velocity space [4, 6, 11], disappears for a 2-D magnetized plasma. This is due to the fact that the magnetic field plays a dominant role in the particle motion. For particle motion along the **B** field, we would still expect recurrence effects. However, for most of the physically interesting cases, the wavelength along the field lines are very large compared to the perpendicular wavelength ($k_\parallel \ll k_\perp$). Therefore, the recurrence time $T_R = 2\pi/(k_\parallel \Delta v_\parallel)$ would be very long for a modest number of grid points in the $v_\parallel$ direction. On the other hand, the recurrence effect can be smoothed out by adding a collision term [12] or other artificial entropy producing term [6] to the system.

Figure 3 shows the power spectrum of 2-D two-species plasma with $k_\parallel \lambda_D = 0$, $k_\perp \lambda_D = 1.414$, $\omega_{ce}/\omega_{pe} = 1$, $T_e/T_i = 1$, $m_i/m_e = 25$. The computation parameters are the same as in Fig. 2. Besides the electron Bernstein modes and dc modes, we

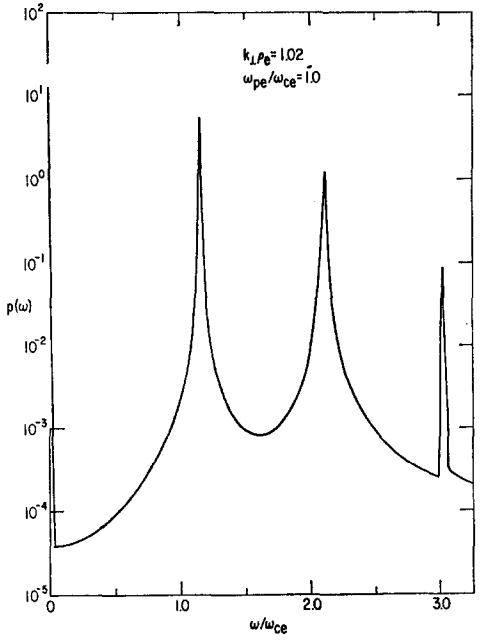

FIG. 2. Power spectrum of the 2-D linearized electron electrostatic waves in a magnetized plasma with $k_\perp \lambda_{De} = 1.02$, $\omega_{ce}/\omega_{pe} = 1$, $k_\parallel \lambda_{De} = 0$.

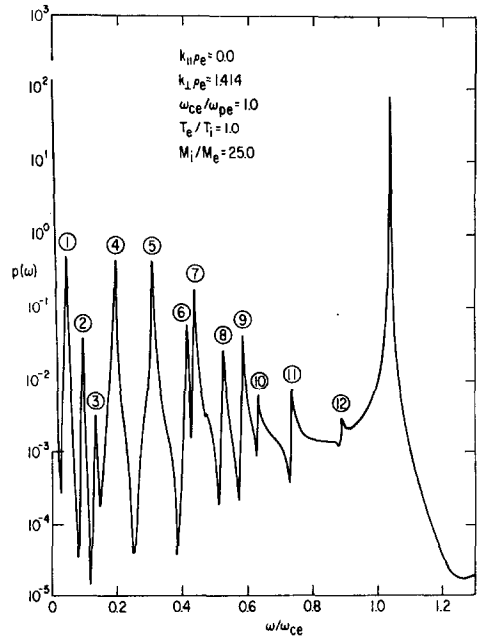

FIG. 3. Power spectrum of the 2-D linearized electrostatic waves in a two-species magnetized plasma with $k_\parallel \lambda_{De} = 0$, $k_\perp \lambda_{De} = 1.414$, $\omega_{ce}/\omega_{pe} = 1$, $T_e/T_i = 1$, $m_i/m_e = 25$.

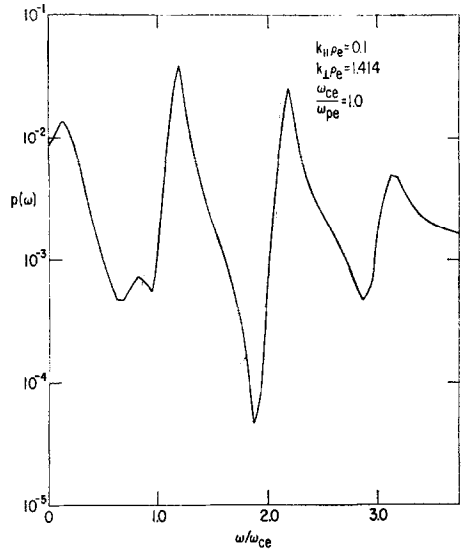

FIG. 4. Power spectrum of the $2\frac{1}{2}$-D linearized electron electrostatic waves in a magnetized plasma with $k_{\parallel}\lambda_{De} = 0.1$, $k_{\perp}\lambda_{De} = 1.414$, $\omega_{ce}/\omega_{pe} = 1$. The peaks are located at $\omega/\omega_{ce} = 0.125$, 0.8125, 1.1875, 2.1875, 3.125.

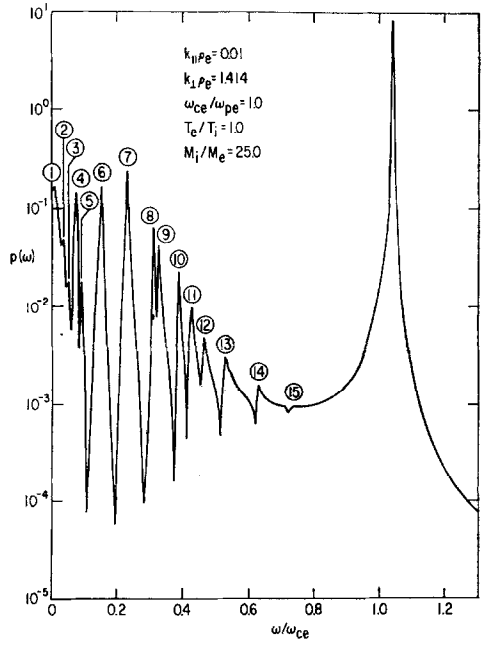

FIG. 5. Power spectrum of the $2\frac{1}{2}$-D linearized electrostatic waves in a two-species magnetized plasma with $k_{\parallel}\lambda_{De} = 0.01$, $k_{\perp}\lambda_{De} = 1.414$, $\omega_{ce}/\omega_{pe} = 1$, $T_e/T_i = 1$, and $m_i/m_e = 25$.

have also obtained the ion Bernstein modes. Figure 4 shows the power spectrum of a $2\frac{1}{2}$-D electron plasma with $k_\parallel \lambda_D = 0.1$, $k_\perp \lambda_D = 1.414$, $\omega_{ce}/\omega_{pe} = 1$. The computation parameters are $N_x = N_y = 4$, $N_\phi = N_r = N_p = 8$, $v_{\perp_{max}} = 4.1$, $v_{\parallel_{max}} = 4.2$, $\omega_{pe}\,\Delta t = \pi/4$. The result agrees very well with Tataronis' linear solutions [13]. Figure 5 shows the power spectrum of a $2\frac{1}{2}$-D, two-species plasma with $k_\parallel \lambda_D = 0.01$, $k_\perp \lambda_D = 1.414$, $\omega_{ce}/\omega_{pe} = 1$, $T_e/T_i = 1$, $m_i/m_e = 25$. The computation parameters are the same as in Fig. 4. For the above computations, the total density, total momentum, and total kinetic energy are conserved except due to roundoff errors.

(B) 2-D *Nonlinear Case*

A 2-D electron plasma with $\omega_{ce}/\omega_{pe} = 1$ has been studied. The initial condition is taken to be

$$f(\mathbf{x}, \mathbf{v}, 0) = 1/2\pi \exp(-v^2/2)(1 + A \cos kx + B \cos ky)$$

where $A = B = 0.01$ and $k\lambda_D = 1.02$. The computation parameters are

$$N_x = N_y = 8, \qquad N_\phi = N_r = 16, \qquad v_{\perp_{max}} = 4.5, \qquad \omega_{pe}\,\Delta t = \pi/8.$$

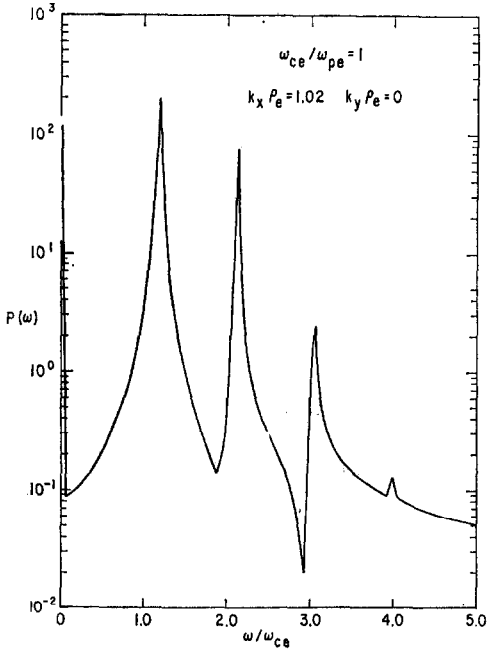

FIG. 6. Power spectrum of the 2-D nonlinear electron electrostatic waves in a magnetized plasma with $k_\parallel = k_y = 0$, $k_x\lambda_{De} = 1.02$, $T_e/T_i = 1$, $m_i/m_e = 25$, and $\omega_{ce}/\omega_{pe} = 1$. The peaks are located at $\omega/\omega_{ce} = 0$, 1.1875, 2.125, 3.0625, 4.0.

We used method 1 described in Section 2 to integrate acceleration Eq. (16) because of the strong magnetic field. Method 1 is superior to method 2 because it separates the fast gyro motion from the slow guiding center drift. If we use method 2, we have to take $\omega_{pe}\,\Delta t$ as small as $\omega_{pe}\,\Delta t = 0.05$ to obtain the same accuracy.

Figures 6 and 7 show the power spectrum and autocorrelation of the potential for (1, 0) mode. The autocorrelation of the potential $\phi(k_\perp, t)$ is defined by $C_{k_\perp}(\tau) = (1/T_{\max}) \int_0^{T_{\max}} \phi(k_\perp, t)\, \phi^*(k_\perp, t - \tau)\, dt$. The computation is carried out for 256 time steps with $\omega_{pe} T_{\max} = 32\pi$. Comparing Figs. 6 and 2, we see that the results of the nonlinear calculation agree very well with the linearized case. The autocorrelation of the potential shows the phase mixing effects of the Bernstein modes, which generate the damping [14] and recurrence phenomena.

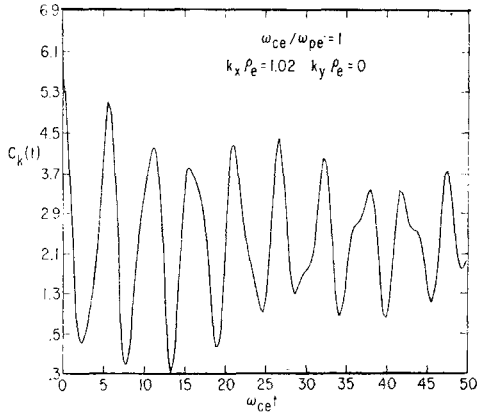

FIG. 7. The autocorrelation of the potential $\phi(k_\perp, t)$ for the nonlinear magnetized electron pasma as in Fig. 6.

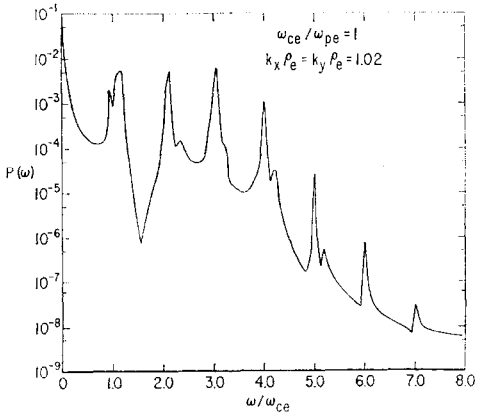

FIG. 8. Power spectrum of (1, 1) mode with $k_\parallel = 0$, $k_x \lambda_{De} = k_y \lambda_{De} = 1.02$. The other parameters are the same as in Fig. 6.

The nonlinear coupling is small; the power spectrum of (1, 1) mode is about a factor 10^{-3} smaller than that of (1, 0) mode and is shown in Fig. 8. The other higher number modes are essentially negligible.

The conservation of the total energy has relative error 10^{-3} at $\omega_{pe}t = 32\pi$. This simulation corresponds to the use of 16384 grid points in the phase space as far as computer storage is concerned. As a reference the computation time is 10 sec per time step for an unoptimized Fortran code on an IBM 360/91. Thus a great saving of computer time is achieved.

4. Conclusion

In this work we have generalized the second-order splitting scheme given by Cheng and Knorr [6] to integrate the three-dimensional, collisionless, magnetized Vlasov system. The resulting free streaming equations are integrated by employing Fourier interpolation as before, but the acceleration equation is integrated by a new splitting scheme, and Gazdag's ASD method and Fourier interpolation are employed to solve the final fractional equations. As a result, the time step Δt can be chosen to be large because the fast gyro motion of the plasma has spearated from the slow guiding center drift and is integrated exactly.

The splitting scheme was tested on the linearized and nonlinear Vlasov equation in 2 D and $2\frac{1}{2}$ D with a Maxwellian equilibrium distribution. The results of these experiments are in very good agreement with the analytic theory. The important feature is not only that the computation time is quite low, but also that good results can be obtained with a few number of grid points. Thus, the 3-D integration of the Vlasov equation can be carried out by using presently available computers.

Acknowledgments

The author would like to thank Drs. H. Okuda and G. Knorr for many helpful discussions. This work was supported by the U. S. Energy Research and Development Administration Contract E(11-1)-3073.

References

1. T. P. Armstrong, R. C. Harding, G. Knorr, and D. Montgomery, *in* "Methods in Computational Physics"(B. Alder, S. Fernbach, and M. Rotenberg, Eds.), Academic Press, New York, 1970. Vol. 9.
2. J. Nührenbery, *J. Appl. Math. Phys.* **22** (1971), 1057.
3. J. Denavit and W. L. Kruer, *Phys. Fluids* **14** (1971), 1782.
4. G. Knorr, *J. Computational Phys.* **13** (1973), 165.
5. H. Gazdag, *J. Computational Phys.* **19** (1975), 77.
6. C. Z. Cheng and G. Knorr, *J. Computational Phys.* **22** (1976), 330.

7. N. N. YANENKO, "The Method of Fractional Steps," Springer–Verlag, New York, 1970.
8. J. GAZDAG, *J. Computational Phys.* **20** (1976), 196.
9. I. B. BERNSTEIN, *Phys. Rev.* **108** (1958), 10.
10. J. Y. HSU AND D. MONTGOMERY, *Phys. Lett. A* **48** (1974), 39.
11. J. CANOSA AND J. GAZDAG, *J. Computational Phys.* **15** (1974), 34.
12. C. E. RATHMANN AND J. DENAVIT, *J. Computational Phys.* **18** (1975), 165.
13. J. A. TATARONIS AND F. W. CRAWFORD, *J. Plasma Phys.* **4** (1970), 231.
14. D. E. BALDWIN AND G. ROWLANDS, *Phys. Fluids* **9** (1966), 2444.